AIP | Applied Physics Letters

Effects of Mn concentration on the ac magnetically induced heating characteristics of superparamagnetic MnxZn1−xFe2O4 nanoparticles for hyperthermia

Minhong Jeun, Seung Je Moon, Hiroki Kobayashi, Hye Young Shin, Asahi Tomitaka et al.

Citation: Appl. Phys. Lett. **96**, 202511 (2010); doi: 10.1063/1.3430043
View online: http://dx.doi.org/10.1063/1.3430043
View Table of Contents: http://apl.aip.org/resource/1/APPLAB/v96/i20
Published by the American Institute of Physics.

Effects of Mn concentration on the ac magnetically induced heating characteristics of superparamagnetic $Mn_xZn_{1-x}Fe_2O_4$ nanoparticles for hyperthermia

Minhong Jeun,[1] Seung Je Moon,[1] Hiroki Kobayashi,[2] Hye Young Shin,[3] Asahi Tomitaka,[2] Yu Jeong Kim,[4] Yasushi Takemura,[2] Sun Ha Paek,[3] Ki Ho Park,[4] Kyung-Won Chung,[5] and Seongtae Bae[1,a)]

[1]*Department of Electrical and Computer Engineering, Biomagnetics Laboratory (BML), National University of Singapore, Singapore 117576*
[2]*Department of Electrical and Computer Engineering, Yokohama National University, Yokohama 240-8501, Japan*
[3]*Department of Neurosurgery, Cancer Research Institute, Ischemic/Hypoxic Disease Institute, Seoul National University College of Medicine, Seoul 110-744, Republic of Korea*
[4]*Department of Ophthalmology, Seoul National University College of Medicine, Seoul 110-744, Republic of Korea*
[5]*Daion Co. Ltd., Incheon 405-846, Republic of Korea*

(Received 8 February 2010; accepted 25 April 2010; published online 21 May 2010)

The effects of Mn^{2+} cation concentration on the ac magnetically induced heating characteristics and the magnetic properties of superparamagnetic $Mn_xZn_{1-x}Fe_2O_4$ nanoparticles (SPNPs) were investigated to explore the biotechnical feasibility as a hyperthermia agent. Among the $Mn_xZn_{1-x}Fe_2O_4$ SPNPs, the $Mn_{0.5}Zn_{0.5}Fe_2O_4$ SPNP showed the highest ac magnetically induced heating temperature ($\Delta T_{ac,mag}$), the highest specific absorption rate (SAR), and the highest biocompatibility. The higher out of phase susceptibility (χ''_m) value and the higher chemical stability systematically controlled by the replacement of Zn^{2+} cations by the Mn^{2+} cations on the *A*-site (tetrahedral site) are the primary physical reason for the promising biotechnical properties of $Mn_{0.5}Zn_{0.5}Fe_2O_4$ SPNP. © *2010 American Institute of Physics*. [doi:10.1063/1.3430043]

Magnetic hyperthermia (MH) using a superparamagntice nanoparticle agent (SPNA) has recently drawn huge attraction due to its clinical promises.[1,2] Accordingly, the interests to utilize the ternary phase of SPNPs, MFe_2O_4 (M=Fe, Co, Ni, and Mg), with a mean diameter below 10 nm for a MH agent has increased dramatically. However, despite their promising chemical, physiological, biotechnical, and physical properties suitable for SPNA applications,[3] an insufficient $\Delta T_{ac,mag}$ and low specific absorption rate (SAR) at the physiologically tolerable range of frequencies and magnetic fields ($f_{appl} < 100$ kHz, $H_{appl} < 200$ Oe) are still revealed as the technical challenges to be overcome for a real clinical MH.[4,5] Thus, a great deal of research activity is being conducted in order to develop a functional SPNA and to improve the efficiency of currently used ferrite SPNAs. The quarterly phase of bulk $Mn_xZn_{1-x}Fe_2O_4$, which is one of the softest (or the highest permeability) ferrite materials, is considered to be a potential material for MH agent. The main physical reason is that it has a good electrical field absorption and a large power loss ($500-200$ W/m^3) at a low frequency (<100 kHz) which is due to its low electrical resistivity ($0.02-20$ Ω m).[6,7] Furthermore, its magnetic properties, i.e., saturation magnetization, M_s, and magnetic susceptibility ($\chi_m = \chi'_m + i\chi''_m$, particularly χ''_m), which are directly relevant to the $\Delta T_{ac,mag}$ characteristics, can be easily controlled by adjusting the relative concentration of Mn^{2+} and Zn^{2+} cations in the $Mn_xZn_{1-x}Fe_2O_4$.[6,8,9] However, all of the works relevant to the $Mn_xZn_{1-x}Fe_2O_4$ done so far were entirely focused on magnetoelectronics device applications.[10] There have been no systematic studies on the magnetic properties, $\Delta T_{ac,mag}$ characteristics, and the biocompatibility of $Mn_xZn_{1-x}Fe_2O_4$ SPNPs for MH agent applications until now.

In this paper, we report on the effects of Mn^{2+} cation concentration on the magnetic properties and the $\Delta T_{ac,mag}$ characteristics of $Mn_xZn_{1-x}Fe_2O_4$ SPNPs to explore its feasibility as a MH agent. The physical correlation between the magnetic properties of $Mn_xZn_{1-x}Fe_2O_4$ SPNPs controlled by the Mn^{2+} cation concentration and $\Delta T_{ac,mag}$, characteristics including power loss mechanism were systematically investigated at different ac H_{appl} and f_{appl}. In addition, the cell viability of $Mn_xZn_{1-x}Fe_2O_4$ SPNPs with different Mn^{2+} cation concentrations were quantitatively analyzed to evaluate the biocompatibility for *in vivo* MH agent applications.

The spinel ferrite $Mn_xZn_{1-x}Fe_2O_4$ nanoparticles (NPs) with different Mn^{2+} cation concentration were synthesized using a modified high temperature thermal decomposition (HTTD) method, where ramping up rate and heat treatment time were changed to 8.5 °C/min and 25 min, respectively, compared to a conventional HTTD method.[11] The Mn^{2+} cation concentration of $Mn_xZn_{1-x}Fe_2O_4$ NPs was systematically controlled from x=0.2 to 0.8 during the synthesis. The crystal structure, the particle size, and the distribution of $Mn_xZn_{1-x}Fe_2O_4$ NPs were analyzed by using a Cu-kα radiated x-ray diffractometer (XRD) and a high resolution transmission electron microscopy (HRTEM). The $\Delta T_{ac,mag}$ characteristics and the ac magnetic hysteresis of the solid state $Mn_xZn_{1-x}Fe_2O_4$ NPs were measured by using an ac solenoid coil system, which is connected to a capacitor. The f_{appl} and the H_{appl} were varied from 30 kHz to 210 kHz and from 60 Oe to 140 Oe, respectively. The dc magnetic properties of the

a)Author to whom correspondence should be addressed. Electronic mail: elebst@nus.edu.sg.

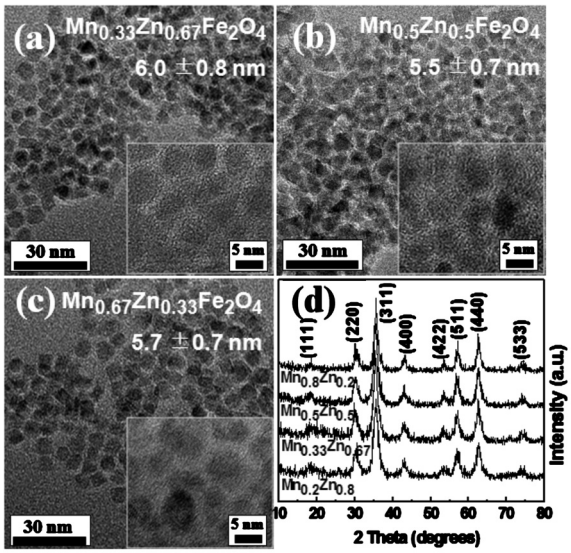

FIG. 1. HRTEM images and XRD patterns of synthesized superparamagnetic $Mn_xZn_{1-x}Fe_2O_4$ nanoparticles with different Mn composition: (a) x =0.33, (b) x=0.5, (c) x=0.67, and (d) XRD patterns.

solid state $Mn_xZn_{1-x}Fe_2O_4$ NPs were analyzed by using a vibrating sample magnetometer and the ac χ_m was measured by using an ac magnetosusceptometer. The zero field cooling/field cooling (ZFC/FC) measurement was carried out to characterize the dependence of temperature on the magnetic properties of $Mn_xZn_{1-x}Fe_2O_4$ NPs using a superconducting quantum interference device (SQUID). The cell viability was quantitatively analyzed by employing the methylthiazol tetrazolium bromide test (MTT) using neuronal stem cells (NSCs) isolated from human fetal midbrain. The $Mn_xZn_{1-x}Fe_2O_4$ NPs were dispersed into the mixed media of 2.5% alcohol, Dulbecco's modified eagle's medium, 10% fetal bovine serum, 1% penicillin streptomycin, and 2 mM glutamine. The concentration of $Mn_xZn_{1-x}Fe_2O_4$ NPs in the media were varied from 5 to 25 μg/ml.

Prior to studying the magnetic properties and the $\Delta T_{ac,mag}$ characteristics, the crystal structure, the particle size and the distribution of $Mn_xZn_{1-x}Fe_2O_4$ NPs were first investigated. As can be seen in Fig. 1, all of the $Mn_xZn_{1-x}Fe_2O_4$ NPs had a mean particle size of 5.7–6 nm with a 12% standard deviation and they were well segregated with a round shapes. In addition, the $Mn_xZn_{1-x}Fe_2O_4$ NPs showed a single phase cubic spinel ferrite structure and did not exhibit any undesirable crystalline phases. The well controlled structural and chemical stabilities of $Mn_xZn_{1-x}Fe_2O_4$ NPs demonstrate that they can be considered to be an *in vivo* MH agent because they are expected to minimize the biochemical reaction with chemical components in the blood stream and to allow for stable intravenous circulation.

Figure 2 shows the hysteresis loops of $Mn_xZn_{1-x}Fe_2O_4$ NPs measured under an externally applied field of (a) $=\pm 10$ kOe and (b) $=\pm 80$ Oe at room temperature. All of the $Mn_xZn_{1-x}Fe_2O_4$ NPs had superparamagnetic (SP) properties. Furthermore, the ZFC/FC measurement results (not shown in this paper) confirmed that the blocking temperature of $Mn_xZn_{1-x}Fe_2O_4$ NPs is in the range of 80–120 K depending on the Mn^{2+} cation concentration, indicating that they have a SP phase at room temperature. As shown in Fig. 2(a), the M_s had a strong dependence on the Mn^{2+} cation concentration. Particularly, the $Mn_{0.5}Zn_{0.5}Fe_2O_4$ NPs had the highest M_s value of a 47 emu/g. The increase in M_s by increasing the Mn^{2+} cation concentration up to x=0.5 is thought to be due to the increase in magnetic moment of the unit cell up to 7.5 μ_B (μ_B: Bohr magneton) which resulted from the replacement of Zn^{2+} ions by Mn^{2+} ions on the *A*-site. However, increasing the Mn^{2+} cation concentration above x=0.5 was found to decrease the M_s. This decrease in M_s is due to the development of antiferromagnetic alignment of Fe^{3+} ions on the *B*-site [see Fig. 3(c)].[6]

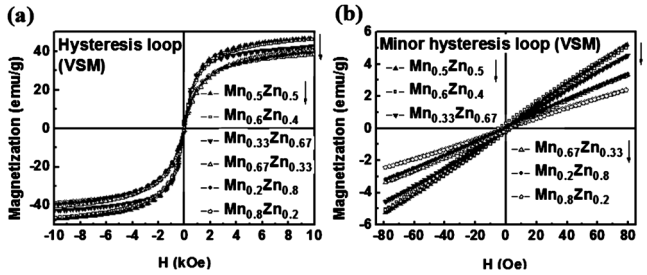

FIG. 2. Magnetic hysteresis loops of $Mn_xZn_{1-x}Fe_2O_4$ nanoparticles with different Mn^{2+} cation concentration changed from x=0.2 to 0.8. (a) Major loop and (b) minor loop.

Figure 3 shows the dependence of Mn^{2+} cation concentration on the $\Delta T_{ac,mag}$ and the magnetic properties of $Mn_xZn_{1-x}Fe_2O_4$ SPNPs. In Fig. 3(a), it can be clearly observed that the $\Delta T_{ac,mag}$ measured at a constant H_{appl} =80 Oe, f_{appl}=210 kHz had a strong dependence on the Mn^{2+} cation concentration. The $\Delta T_{ac,mag}$ of $Mn_xZn_{1-x}Fe_2O_4$ SPNPs was increased by increasing the Mn concentration and reached a maximum $\Delta T_{ac,mag}=39$ °C at the composition of $Mn_{0.5}Zn_{0.5}Fe_2O_4$. A further increase in Mn concentration, x>0.5, led to a severe reduction in $\Delta T_{ac,mag}$. The physical dependence of f_{appl} and H_{appl} on the $\Delta T_{ac,mag}$ is shown in Fig. 3(b). It was clearly demonstrated that the $\Delta T_{ac,mag}$ is linearly proportional to the f_{appl} and squarely proportional to the H_{appl}. These results strongly imply that the physical nature of $\Delta T_{ac,mag}$ of $Mn_xZn_{1-x}Fe_2O_4$

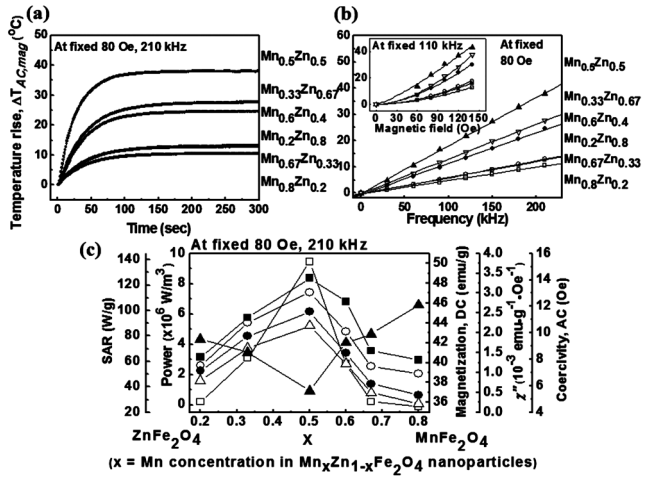

FIG. 3. Dependence of Mn^{2+} cation concentration on the (a) ac magnetically induced heating characteristics measured at the fixed H_{appl}=80 Oe and f_{appl}=210 kHz, (b) applied frequency and magnetic field, and (c) SAR, heating power (total and relaxation loss), magnetization, out of phase susceptibility and ac magnetic coercivity of superparamagnetic $Mn_xZn_{1-x}Fe_2O_4$ nanoparticles [□ SAR, ■ magnetization (dc), ○ P_{total}, ● $P_{relaxation\ loss}$, △ ac susceptibility, and ▲ coercivity (ac)].

SPNPs is dominantly related to the "relaxation loss" heating power, $P_{\text{relaxation loss}}$, as described in Eqs. (1) and (2).[12] Furthermore, from this point of view, the highest $\Delta T_{ac,mag}$ value obtained from the $Mn_{0.5}Zn_{0.5}Fe_2O_4$ SPNP can be understood to be due to its highest measured χ''_m value which resulted from its softest magnetic property as well as its largest exchange energy induced by the half portion of Zn^{2+} ions replaced by the Mn^{2+} ions on the *A*-site.

$$P_{\text{relaxation loss}} = \pi\mu_0\chi''_m f_{\text{appl}} H^2_{\text{appl}}, \tag{1}$$

$$\chi'' = \chi_0 \frac{2\pi f\tau}{1+(2\pi f\tau)^2}, \frac{1}{\tau} = \frac{1}{\tau_N} + \frac{1}{\tau_B} \approx \frac{1}{\tau_N}$$
$$= \frac{2\sqrt{K_u V/k_B T}}{\sqrt{\pi}\cdot\tau_0 \exp(K_u V/k_B T)}, (\text{soft ferrite}: \tau_N \ll \tau_B), \tag{2}$$

where τ_N: Néel relaxation time, τ_B: Brownian relaxation time, τ_0:relaxation factor, and K_u: magnetic anisotropy.

The ac magnetic coercivity of $Mn_xZn_{1-x}Fe_2O_4$ SPNPs measured at $H_{\text{appl}} = \pm 80$ Oe and $f_{\text{appl}} = 210$ kHz is shown in Fig. 3(c). The $Mn_{0.5}Zn_{0.5}Fe_2O_4$ SPNP exhibited the smallest ac magnetic coercivity among the $Mn_xZn_{1-x}Fe_2O_4$ SPNPs indicating that it has the lowest ac magnetic anisotropy resulting in the fastest τ_N [or the highest χ''_m described in Eq. (2)]. This experimental result provides strong physical evidence that the highest $\Delta T_{ac,mag}$ of $Mn_{0.5}Zn_{0.5}Fe_2O_4$ SPNP (x=0.5) is related directly to the well-controlled highest χ''_m. Furthermore, this indicates that controlling the ac magnetic softness of SPNPs, which is directly relevant to the Néel relaxation behavior, is the most crucial factor in determining the $\Delta T_{ac,mag}$ characteristics. In order to further clarify the physical mechanism of $\Delta T_{ac,mag}$ of $Mn_xZn_{1-x}Fe_2O_4$ SPNPs, the contribution of $P_{\text{relaxation loss}}$ to the total power heat generation, P_{total}, was numerically compared by calculating both P_{total} and $P_{\text{relaxation loss}}$ from the experimentally obtained $\Delta T_{ac,mag}$, χ''_m (at $f_{\text{appl}} = 210$ kHz), mass, and the volumetric heat capacity values of $Mn_xZn_{1-x}Fe_2O_4$ SPNPs. As can be seen in Fig. 3(c), more than 80% or 90% of $P_{\text{relaxation loss}}$ contributed to the P_{total} of $Mn_xZn_{1-x}Fe_2O_4$ SPNPs verifying that the $P_{\text{relaxation loss}}$, particularly the Néel relaxation power loss is dominant for the $\Delta T_{ac,mag}$ of $Mn_xZn_{1-x}Fe_2O_4$ SPNPs. To consider the SPNPs for a real clinical MH agent without systemic side effect, the SPNPs should generate a higher $\Delta T_{ac,mag}$ both in a short heat up time and with a amount as low as possible. These characteristics can be evaluated by the SAR shown in Fig. 3(c).[13] The $Mn_{0.5}Zn_{0.5}Fe_2O_4$ SPNP showed the largest SAR value of 138.4 W/g due to the fastest temperature rising rate ($\Delta T/\Delta t$) caused by the highest χ'' value among the $Mn_xZn_{1-x}Fe_2O_4$ SPNPs. This value is considered to be much higher than those obtained from the conventional ternary phase SPNAs at the same ac condition, e.g., Fe_3O_4 (27.3 W/g), $CoFe_2O_4$ (56.1 W/g), and $NiFe_2O_4$ (12.6 W/g).[14]

The cell viability of $Mn_xZn_{1-x}Fe_2O_4$ SPNPs with different concentrations was quantitatively estimated to explore the feasibility to a MH agent particularly targeted for brain tumors. Figure 4 showed the cell survival rate treated for (a) one day and (b) two weeks, respectively. It was clearly confirmed that the cell survival rate of $Mn_xZn_{1-x}Fe_2O_4$ SPNPs

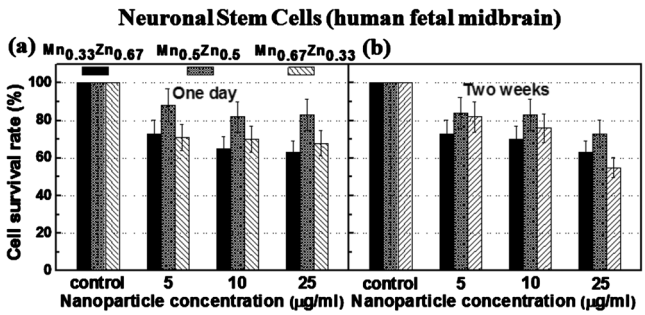

FIG. 4. Cell viability of superparamagnetic $Mn_xZn_{1-x}Fe_2O_4$ nanoparticles (x=0.33, 0.5, and 0.67) in MTT assay with NSCs isolated from human fetal midbrain treated for (a) one day and (b) two weeks.

depends on the concentration of NPs in the cell culture media as well as the Mn^{2+} cation concentration. All three SPNPs showed midcytotoxicity or noncytotoxicity. In particular, the $Mn_{0.5}Zn_{0.5}Fe_2O_4$ SPNP had the highest cell survival rate of 80% ± 8% (10% of standard deviation) even at a higher NP concentration and for a long treatment time. The higher cell survival rate of $Mn_{0.5}Zn_{0.5}Fe_2O_4$ SPNP is thought to be due to the chemically stable phase of $Mn_{0.5}Zn_{0.5}Fe_2O_4$, which is expected to induce less stress on the cells and the large portion of Mn^{2+} cation concentration, which is considered to have a high biocompatibility.[15]

In conclusion, it was demonstrated that the $\Delta T_{ac,mag}$ and the magnetic properties of $Mn_xZn_{1-x}Fe_2O_4$ SPNPs had a strong dependence on the Mn^{2+} cation concentration. Among the $Mn_xZn_{1-x}Fe_2O_4$ SPNPs, the $Mn_{0.5}Zn_{0.5}Fe_2O_4$ SPNP showed the highest $\Delta T_{ac,mag}$, SAR, and biocompatibility, which make it suitable for MH agent applications. The higher χ'' value directly relevant to the τ_N (or ac magnetic softness) and the higher chemical stability systematically controlled by the replacement of Zn^{2+} cations by the Mn^{2+} cations on the *A*-site are the primary physical reason for the biotechnical promises of $Mn_{0.5}Zn_{0.5}Fe_2O_4$ SPNP.

[1] P. Moroz, S. K. Jones, and B. N. Gray, Int. J. Hyperthermia **18**, 267 (2002).
[2] Q. A. Pankhurst, N. K. T. Thanh, S. K. Jones, and J. Dobson, J. Phys. D: Appl. Phys. **42**, 224001 (2009).
[3] S. Bae, S. W. Lee, and Y. Takemura, Appl. Phys. Lett. **89**, 252503 (2006).
[4] P. Wust, U. Gneveckow, U. M. Johannsen, D. Böhmer, T. Henkel, F. Kahmann, J. Sehouli, R. Felix, J. Ricke, and A. Jordan, Int. J. Hyperthermia **22**, 673 (2006).
[5] K. Okawa, M. Sekine, M. Maeda, M. Tada, and M. Abe, J. Appl. Phys. **99**, 08H102 (2006).
[6] A. Goldman, *Modern Ferrite Technology* (Springer, New York, 2006).
[7] M. Sugimoto, J. Am. Ceram. Soc. **82**, 269-80 (1999).
[8] R. E. Rosensweig, J. Magn. Magn. Mater. **252**, 370 (2002).
[9] Y. Xuan, Q. Li, and G. Yang, J. Magn. Magn. Mater. **312**, 464 (2007).
[10] C. Rath, K. K. Sahu, S. Anand, S. K. Date, N. C. Mishra, and R. P. Das, J. Magn. Magn. Mater. **202**, 77 (1999).
[11] S. Sun, H. Zeng, D. B. Robinson, S. Raoux, P. M. Rice, S. X. Wang, and G. Li, J. Am. Chem. Soc. **126**, 273 (2004).
[12] M. Gonzales and K. M. Krishnan, J. Magn. Magn. Mater. **293**, 265 (2005).
[13] T. Hosono, H. Takahashi, A. Fujita, R. J. Joseyphus, K. Tohji, and B. Jeyadevan, J. Magn. Magn. Mater. **321**, 3019 (2009).
[14] S. W. Lee, S. Bae, M. Jeun, T. Koshi, and Y. Takemura, 53rd Annual Conference on Magnetism and Magnetic Materials, Texas, CG-14, 2008.
[15] E. John, *An A-Z Guide to the Elements* (Oxford University Press, Oxford, 2001).